Acta Crystallographica Section F
Structural Biology and Crystallization Communications
ISSN 1744-3091

Antigen recognition by antibody C836 through adjustment of V_L/V_H packing

Alexey Teplyakov,* Galina Obmolova, Thomas Malia and Gary Gilliland

Centocor R&D Inc., 145 King of Prussia Road, Radnor, PA 19087, USA

Correspondence e-mail: ateplyak@its.jnj.com

Received 9 June 2011
Accepted 11 July 2011

PDB Reference: C836 Fab, 3l7e.

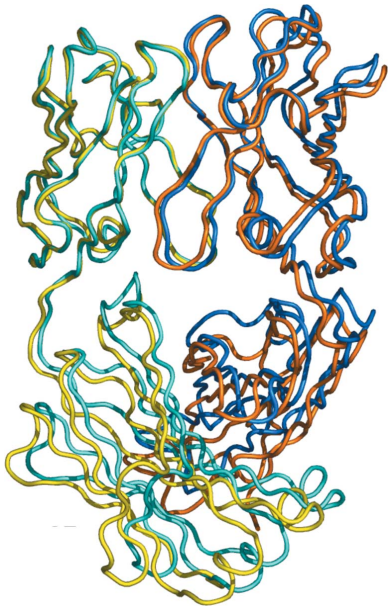

C836 is a neutralizing monoclonal antibody to human interleukin IL-13 generated by mouse immunization. The crystal structure of the C836 Fab was determined at 2.5 Å resolution and compared with the IL-13-bound form determined previously. This comparison indicates an induced-fit mechanism of antigen recognition through rigid-body rotation of the V_L and V_H domains. The magnitude of this rearrangement is one of the largest observed for antibody–protein interactions.

1. Introduction

The Fab fragments of antibodies are heterodimers composed of heavy and light chains, each folded into variable and constant domains. All four domains share the β-sandwich topology known as the immunoglobulin fold (Bork *et al.*, 1994). The antigen-recognition site is composed of complementarity-determining regions (CDRs) located within the loops of the variable domains V_L and V_H. While most antibodies operate by the key-and-lock mechanism, others undergo considerable rearrangement upon antigen binding (Colman, 1988). Early structural studies documented induced-fit movements in antibodies that can involve rearrangement of side chains, backbone shifts of CDRs and changes in the relative disposition of the V_L and V_H domains (Bhat *et al.*, 1990; Stanfield *et al.*, 1990, 1993; Herron *et al.*, 1991; Rini *et al.*, 1992).

Comparison of the structures of Fabs in their free and bound states expands our knowledge of the mechanisms underlying antigen recognition. There are nearly 1000 entries in the Protein Data Bank (Bernstein *et al.*, 1977) containing Fabs and Fab–antigen complexes. However, very few antibodies have been crystallized in both the bound and unbound states. These data provide useful information on the structural determinants of antibody flexibility and adaptability that can be utilized in antibody engineering. With this in mind, we have determined the crystal structure of the C836 Fab in the free state in order to enable comparison with the antigen-bound form determined previously (Fransson *et al.*, 2010).

C836 is a neutralizing monoclonal antibody to human interleukin IL-13 generated by mouse immunization. C836 has demonstrated efficacy in experimental models of asthma (Yang *et al.*, 2004). Previously, we determined the crystal structure of the IL-13–C836 complex (PDB entry 3l5w) and identified residues involved in antibody–antigen interactions (Fransson *et al.*, 2010). Comparison of the free and IL-13-bound forms of the Fab indicates an induced-fit mechanism of antigen recognition through rigid-body rotation of the V_L and V_H domains. The magnitude of this rearrangement is one of the largest observed for antibody–protein interactions.

2. Experimental methods

2.1. Crystallization

The Fab fragment of chimeric C836 (mouse variable domain and human IgG1/κ constant domain) with a six-His tag at the C-terminus of the heavy chain was expressed in HEK cells and purified using affinity and size-exclusion chromatography (Teplyakov *et al.*, 2010).

Table 1
X-ray data and refinement statistics.

Values in parentheses are for the highest resolution shell.

X-ray data	
Resolution (Å)	20–2.5 (2.6–2.5)
No. of unique reflections	30327 (2429)
Completeness (%)	94.8 (75.7)
Multiplicity	7.7 (7.0)
R_{merge}†	0.080 (0.408)
$\langle I/\sigma(I)\rangle$	10.4 (3.0)
B factor (Wilson plot) (Å^2)	59.8
Refinement	
Resolution (Å)	15–2.5
No. of atoms	6748
No. of water molecules	174
R factor‡	0.201
R_{free}‡ (5% of data)	0.251
R.m.s. deviations	
Bond lengths (Å)	0.009
Bond angles (°)	1.3
Ramachandran plot favored§ (%)	96.2
Ramachandran plot outliers§ (%)	0.3
Mean *B* factor (Å^2)	45.9

† $R_{merge} = \sum_{hkl}\sum_i |I_i(hkl) - \langle I(hkl)\rangle| / \sum_{hkl}\sum_i I_i(hkl)$, where $I_i(hkl)$ is the intensity of the *i*th observation of unique reflection *hkl* and $\langle I(hkl)\rangle$ is the average intensity. ‡ $R = \sum_{hkl} ||F_{obs}| - |F_{calc}|| / \sum_{hkl} |F_{obs}|$, where F_{obs} are the observed and F_{calc} are the calculated structure factors. § As defined in *MolProbity* (Chen *et al.*, 2010).

The Fab was crystallized by the vapor-diffusion sitting-drop method at 293 K using a Hydra II eDrop robot (Thermo Scientific). Initial screening was performed with Crystal Screen (Hampton Research) and in-house crystallization screens and was followed by optimization screening. X-ray-quality Fab crystals grew from 16%(*w*/*v*) PEG 4000, 0.2 *M* ammonium sulfate, 0.1 *M* sodium acetate pH 4.5. They belonged to the monoclinic space group *C*2, with unit-cell parameters a = 97.94, b = 141.46, c = 76.58 Å, β = 117.46°. The asymmetric unit contained two Fab molecules.

2.2. Structure determination and analysis

X-ray diffraction data were collected on a Rigaku MicroMax-007 HF X-ray generator equipped with a Saturn 944 CCD detector and an X-stream 2000 cryocooling system. The Fab crystal was soaked for a few seconds in mother liquor supplemented with 20% glycerol and flash-frozen in a stream of nitrogen at 100 K. Diffraction intensities were collected over a 360° crystal rotation with an exposure time of 120 s per 0.5° image. The data were processed with the program *d*TREK* (Rigaku). X-ray data statistics are given in Table 1.

The structure was determined by molecular replacement using the program *MOLREP* (Vagin & Teplyakov, 2010) with the structure of anti-carbohydrate antibody S25-2 (PDB entry 1q9q; Nguyen *et al.*, 2003) as a search model. The structure was refined with *REFMAC* (Murshudov *et al.*, 2011) using all data in the resolution range 15–2.5 Å. The refinement statistics are given in Table 1. All crystallographic calculations were performed with the *CCP*4 suite of programs (Winn *et al.*, 2011). Model adjustments were carried out using the program *Coot* (Emsley & Cowtan, 2004). All molecular illustrations were prepared with *PyMOL* (DeLano, 2002).

The elbow angle, the angle between the two pseudo-dyad axes of the variable (V_L + V_H) and the constant (C_L + C_{H1}) domains, was calculated with the program *RBOW* (Stanfield *et al.*, 2006). The V_L/V_H packing angle is measured between the axes of V_L and V_H. The change in the V_L/V_H packing angle between two structures was calculated by sequential superposition of C^α atoms of the residues forming the β-structure, first in the V_L domain (residues 3–13, 19–26, 32–38, 45–49, 53–55, 61–67, 70–76, 84–91 and 97–105) and then in the V_H domain (residues 3–12, 16–25, 33–39, 46–52, 56–60, 66–72, 77–82, 88–95 and 102–111). The rotation angle χ in polar coordinates of the second transformation is the change in the packing angle.

The atomic coordinates and structure factors for the free C836 Fab have been deposited in the PDB under accession code 3l7e.

3. Results and discussion

The C836 Fab structure was determined at 2.5 Å resolution. All CDR residues are clearly visible in the electron density, indicating that there are no disordered regions in the antigen-binding loops. There are two copies of the Fab in the asymmetric unit and their structures are virtually identical based on separate superposition of the variable and constant domains (r.m.s.d.s of 0.36 and 0.37 Å, respectively). The elbow angles between the variable and constant domains are 136.3° and 138.7° in the two independent Fab molecules. In the IL-13 complex the Fab elbow angles are 141.2° and 143.6°, *i.e.* close to the values in the free Fab (Fig. 1). This comparison shows that the quaternary structure of C836 Fab is rigid enough to withstand crystal lattice forces. The observed range of elbow angles for IgG1/κ antibodies spans 70° from 124° to 194° (Stanfield *et al.*, 2006).

Superposition of the free Fab (this structure) on the IL-13 complex (PDB entry 3l5w) shows that antigen binding causes some noticeable changes in the CDRs. Superposition of the variable domains (V_L + V_H) gives an r.m.s. deviation of 0.59 Å for C^α atoms. A separate superposition of the V_L and V_H regions gives much smaller deviations of 0.38 and 0.37 Å, respectively, indicating a change in the relative packing of V_L and V_H. The difference in the packing angle is 5°, which appears to be one of the largest among structures deposited in the PDB. We have found two other examples in which binding of the protein antigen caused a change in the packing angle of a similar magnitude. An early case was described by Ban *et al.* (1995), in which an anti-idiotypic antibody underwent a 5° rotation of the variable domains upon binding the target antibody (PDB entries 1aif and

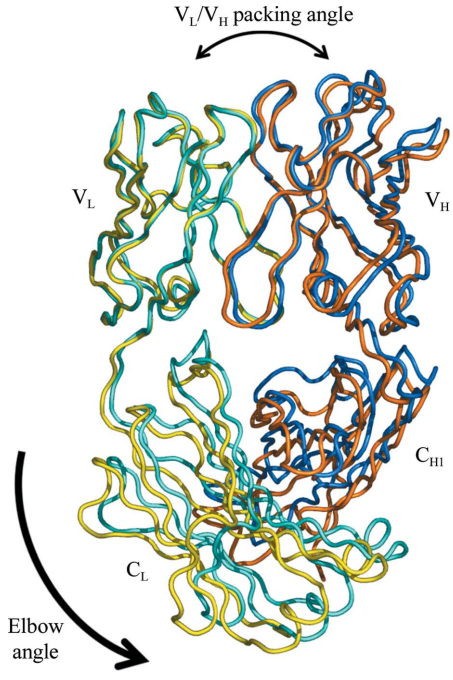

Figure 1
C836 Fab structures in the free state (light chain, cyan; heavy chain, blue) and in the complex (light chain, yellow; heavy chain, orange) superimposed on the V_L domains.

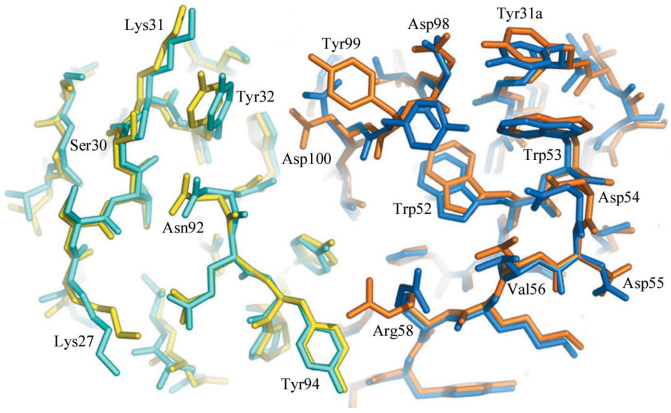

Figure 2
Superposition of the C836 variable domains in the free state (V_L, cyan; V_H, blue) and in the complex (V_L, yellow; V_H, orange). Residues are numbered according to Chothia & Lesk (1987).

1iai). Another example is antibody ATN615, which exhibits a relative rotation of V_L and V_H of 7° upon association with urokinase plasminogen activator receptor (PDB entries 2fat and 2fd6; Li *et al.*, 2007). Typically, the packing angle does not change by more than 1–2°, which is often within the accuracy of structure determination. However, there are always exceptions, and C836 seems to be one of them.

The relative movement of the V_L and V_H domains upon binding IL-13 opens the antigen-recognition cleft by 1 Å as measured between the tips of CDR L1 (Ser30) and CDR H2 (Asp54) (Fig. 2). Without this adjustment, the interactions between Trp52, Trp53 and Asp54 of CDR H2 and IL-13 would be suboptimal. This relatively small but significant main-chain shift may account for the high binding affinity of the antibody (K_d = 50 p*M*) that might be difficult to achieve by other means given the small recognition area of C836 (620 Å^2).

Besides the backbone shifts in the CDRs caused by the V_L/V_H rotation, a number of residues in direct contact with IL-13 change their rotamers (Fig. 2). These include Asp98, Tyr99 and Asp100 in CDR H3 and Arg58 in CDR H2, all of which exhibit rotations around $C^{\alpha}-C^{\beta}$ bonds upon complex formation. This is not a crystallographic artifact since all these residues are not involved in crystal contacts that might affect their conformation. Importantly, their conformation in the free Fab is not compatible with the position of IL-13 in the complex.

Since the bound and unbound forms of the Fab were crystallized at different pH values (the free Fab at pH 4.5 and the complex at pH 7.5), we investigated whether this could have affected the quaternary structure. The difference of three pH units suggests that some amino acids, particularly histidine, may be in different protonation states. There are two histidine residues in the variable domain, His91 in V_L and His50 in V_H, and both are close to the V_L/V_H interface. His50 does not form hydrogen bonds and therefore is unlikely to impact on the interactions. His91 of CDR L3 forms a hydrogen bond to Asp100 of CDR H3 in the complex but not in the free Fab. If the pH shift was the cause of the difference, one would expect the opposite, as the fully protonated histidine in the free Fab would be a better hydrogen donor. It seems that the rearrangement of CDR H3 including Asp100 is a prerequisite for the association with IL-13, which has probably nothing to do with the protonation of His91.

Comparison of the IL-13-bound and unbound forms of C836 Fab indicates that this antibody employs an induced-fit mechanism of antigen recognition. However, the adjustment of the antigen-binding loops is achieved not through their local conformational rearrangement but rather through rigid-body rotation of the V_L and V_H domains and side-chain rotation of key interacting residues. This example illustrates the diverse repertoire of antigen-recognition mechanisms utilized by antibodies. Targeting the V_L/V_H packing angle may prove to be a useful approach for antibody engineering.

Computational methods aimed at modeling the antigen-binding sites of antibodies have achieved a certain reliability in predicting the conformation of five out of the six CDRs (with CDR H3 being the exception). Recently, it has been appreciated that variation in V_L/V_H packing should be taken into account and several algorithms based on analysis of interface residues have been developed (Narayanan *et al.*, 2009; Sivasubramanian *et al.*, 2009; Abhinandan & Martin, 2010). These efforts will undoubtedly enhance antibody-engineering techniques, particularly the framework selection and library design in the humanization process. However, prediction of the tertiary and quaternary changes that can occur upon antigen binding remains a problem. Accumulation of structural data may help to solve this problem in the future.

References

Abhinandan, K. R. & Martin, A. C. (2010). *Protein Eng. Des. Sel.* **23**, 689–697.
Ban, N., Escobar, C., Hasel, K. W., Day, J., Greenwood, A. & McPherson, A. (1995). *FASEB J.* **9**, 107–114.
Bernstein, F. C., Koetzle, T. F., Williams, G. J., Meyer, E. F. Jr, Brice, M. D., Rodgers, J. R., Kennard, O., Shimanouchi, T. & Tasumi, M. (1977). *J. Mol. Biol.* **112**, 535–542.
Bhat, T. N., Bentley, G. A., Fischmann, T. O., Boulot, G. & Poljak, R. J. (1990). *Nature (London)*, **347**, 483–485.
Bork, P., Holm, L. & Sander, C. (1994). *J. Mol. Biol.* **242**, 309–320.
Chen, V. B., Arendall, W. B., Headd, J. J., Keedy, D. A., Immormino, R. M., Kapral, G. J., Murray, L. W., Richardson, J. S. & Richardson, D. C. (2010). *Acta Cryst.* D**66**, 12–21.
Chothia, C. & Lesk, A. M. (1987). *J. Mol. Biol.* **196**, 901–917.
Colman, P. M. (1988). *Adv. Immunol.* **43**, 99–132.
DeLano, W. L. (2002). *PyMOL*. http://www.pymol.org.
Emsley, P. & Cowtan, K. (2004). *Acta Cryst.* D**60**, 2126–2132.
Fransson, J. *et al.* (2010). *J. Mol. Biol.* **398**, 214–231.
Herron, J. N., He, X. M., Ballard, D. W., Blier, P. R., Pace, P. E., Bothwell, A. L., Voss, E. W. Jr & Edmundson, A. B. (1991). *Proteins*, **11**, 159–175.
Li, Y., Parry, G., Chen, L., Callahan, J. A., Shaw, D. E., Meehan, E. J., Mazar, A. P. & Huang, M. (2007). *J. Mol. Biol.* **365**, 1117–1129.
Murshudov, G. N., Skubák, P., Lebedev, A. A., Pannu, N. S., Steiner, R. A., Nicholls, R. A., Winn, M. D., Long, F. & Vagin, A. A. (2011). *Acta Cryst.* D**67**, 355–367.
Narayanan, A., Sellers, B. D. & Jacobson, M. P. (2009). *J. Mol. Biol.* **388**, 941–953.
Nguyen, H. P., Seto, N. O., MacKenzie, C. R., Brade, L., Kosma, P., Brade, H. & Evans, S. V. (2003). *Nature Struct. Biol.* **10**, 1019–1025.
Rini, J. M., Schulze-Gahmen, U. & Wilson, I. A. (1992). *Science*, **255**, 959–965.
Sivasubramanian, A., Sircar, A., Chaudhury, S. & Gray, J. J. (2009). *Proteins*, **74**, 497–514.
Stanfield, R. L., Fieser, T. M., Lerner, R. A. & Wilson, I. A. (1990). *Science*, **248**, 712–719.
Stanfield, R. L., Takimoto-Kamimura, M., Rini, J. M., Profy, A. T. & Wilson, I. A. (1993). *Structure*, **1**, 83–93.
Stanfield, R. L., Zemla, A., Wilson, I. A. & Rupp, B. (2006). *J. Mol. Biol.* **357**, 1566–1574.
Teplyakov, A., Obmolova, G., Carton, J. M., Gao, W., Zhao, Y. & Gilliland, G. L. (2010). *Mol. Immunol.* **47**, 2422–2426.
Vagin, A. & Teplyakov, A. (2010). *Acta Cryst.* D**66**, 22–25.
Winn, M. D. *et al.* (2011). *Acta Cryst.* D**67**, 235–242.
Yang, G., Volk, A., Petley, T., Emmell, E., Giles-Komar, J., Shang, X., Li, J., Das, A. M., Shealy, D., Griswold, D. E. & Li, L. (2004). *Cytokine*, **28**, 224–232.